LUNAR LANDING SITE LOCALIZATION, TRAJECTORY INVERSION AND DTM UPDATE FROM CHANG'E-3 DESCENT IMAGES. R. Binet[1], M.Grizonnet[1], A.Torres[1], J-C. Malapert[1], F. Jocteur-Moronzier[1], [1]CNES (11 av. Edouard Belin, Toulouse 31400, France, renaud.binet@cnes.fr).

Introduction: In the frame of CNES support to Team Indus moon landing project [1], an image processing pipeline based on lander descent images has been setup in order to determine precisely the landing site localization, to update the DTM in the vicinity of the landing site, and provide mosaics of orthoimages in a ground reference frame.

These objectives are motivated by the rover path planning operations [2] : the rover path planning is precomputed before launch and is updated relatively to the lander localization. The relative localization of the lander within the reference LRO NAC image must be known with an accuracy better than 20m. It can be estimated by intersecting an estimated trajectory with the ground. We propose to estimate the trajectory from the descent images and a reference image and DTM, actually LRO NAC data.

Beside, a DTM update is meaningful to prevent from rover-lander communications line of sight masking and strong slopes. An update of the DTM enables a refinement of the rover path provided a better accuracy is obtained by processing the descent images in a stereoscopic reconstruction fashion.

Structure From Motion (SFM) algorithms [3] are well known for their ability to estimate 3D positions and shape of objects given a set of images from the same camera with different points of view. As a prerequisite, SFM algorithms estimate also the relative motion of the camera as well as the inner parameters of the camera itself. We propose to evaluate the ability of SFM processing to estimate the trajectory of the lander and the DTM reconstruction. Touchdown location is then given by the intersection of the extrapolated descent trajectory with the DTM. Here we state that images are available until touchdown so that no extrapolation is needed.

The accuracy of SFM algorithms depends strongly on the image content. In particular, smooth surfaces are hard to render because the image matching process inherent to SFM fails on textureless areas. Therefore a test on real images is highly preferred to simulated images. Hopefully this opportunity is given by Chang'e-3 data which have been released in the public domain in 2015 [4]. In particular the descent camera LCAM is similar to the LDS camera that will be used on Team Indus lander. Another question raised by these data is the DTM accuracy that can be obtained in such poorly constrained stereoscopic configuration.

We present hereafter the results obtained with Chang'e-3 LCAM images : trajectory inversion, lander localization, and DTM evaluation.

Data set :

LCAM dataset : LCAM, mounted at the bottom of the lander, obtained image data during the lander descent from an elevation range of 12 km to touchdown. Level 2A has been used for this study. Images are only corrected from detectors non uniformity. Imaging frequency of LCAM is 1Hz. We undersampled the image sequence to 20s time interval in order to limit the computation time. A total of 175 images have been processed. The initial focal length is set to 8.5mm. The field of view is 45.3°x45.3° on an effective grid of 1024x1024 pixels. The pixel pitch is 6.7µm. We did not use any other information such as lander navigation data or camera calibration parameters.

LRO reference data: LRO data are used as absolute geographical reference in the processing pipeline. We used a NAC DTM (5m pitch) and a NAC orthoimage (1,5m pitch) centered on the Chang'e-3 landsite. We selected 9 ground control points (GCPs) manually between NAC images and LCAM images.

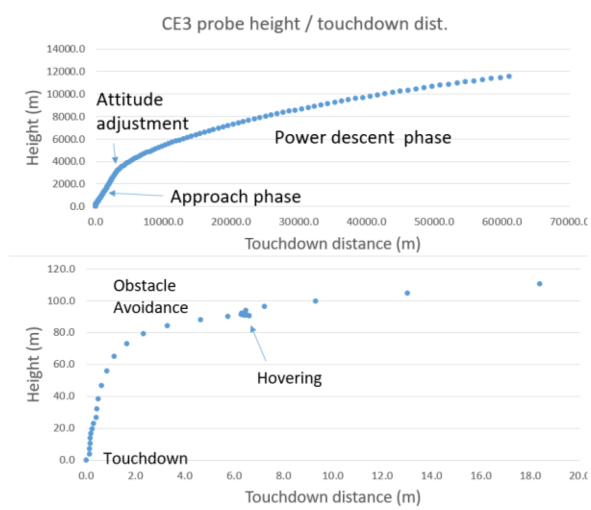

Figure 1 : Mission analysis from trajectory inversion

Processing tool: Numerous SFM tools are candidate for handling such image processing. After trying Agisoft Photoscan without success, we selected Micmac software suite [5], an open source solution suited to a great number of 3D applications and scales (aerial, drone, satellite, hand camera, etc.). Micmac enables control of the data at each step of the process, which is not always the case with commercial solutions.

Trajectory inversion processing: the first step is an automatic tie point selection (SIFT tie points) and matching between all images pair limited to an image interval of 10. A mask has been applied to pixels belonging to elements of the lander and a local contrast enhancement has been applied in order to increase the number of tie points. At step 2, a fine estimation of camera calibration parameters is set by a bundle adjustment based on a selected set of images. At this step, in order to prevent poorly constrained inversion, one shall prefer images for which the speed direction is not colinear to the main line of sight. We found a focal length of 8.29mm, in good accordance with the 8.5mm initial value found in [6]. In step 3, the images relative positions and orientations are computed thanks to a global bundle adjustment involving all images. Without initial estimates of the camera relative positions, an initial guess is built with an iterative processing tying one image on the others successively. This processing tends to propagates errors and cannot handle all images in such a linear sketch. We then processed sets of 30 images with 10 common images for each set. Then we merged the sets of orientations in order to get the whole initial relative orientations. At this step, the residuals of tie points are 0.4 pixel rms, for an average number of 5000 tie points per image. We then introduce GCPs taken on LRO NAC images in order to set the scale and the absolute orientations of the images. A final bundle adjustment is done with all the images and these GCPs altogether. The result is a set of absolute positions and orientations for each image, acquired from 12km altitude to touchdown.

Touchdown location is given by the last image position. Discrepancy with the location given by a NAC image where CE3 is seen is less than 1m.

Numerous proxies can be computed for mission analysis, such as trajectory, attitude and speed profiles during the whole descent. We have been able to monitor all descent sequences of Chang'e-3 lander : power descent, attitude adjustment phase, approach phase, hovering, obstacle avoidance, and final low speed descent. Positions computed are in very good accordance with [7] and [8]. Figure 1 shows the trajectory height profile w.r.t touchdown distance in which the sequences are clearly identifiable. In particular avoidance manoeuver is estimated to 6m.

DTM reconstruction: given the set of oriented images, the DTM can be estimated by conventional stereoscopic algorithms. Because the image resolution and swath is continuously decreasing with time, DTM accuracy depends mostly on the images selected for the DTM estimation. We present in figure 2 the comparison of the larger scale DTM computation with the NAC reference DTM. Small craters are revealed in our DTM that are not visible in NAC DTM. We also notice block artefacts in NAC DTM. A global E-W slope is also noticed in our DTM due to a lack of GCPs across track. Figure 3 shows the DTM obtained at finer scale with images height under 800m (respectively 115m).

Such a method could also prove to be useful in forthcoming missions such as Mars 2020 or even DragonFly.

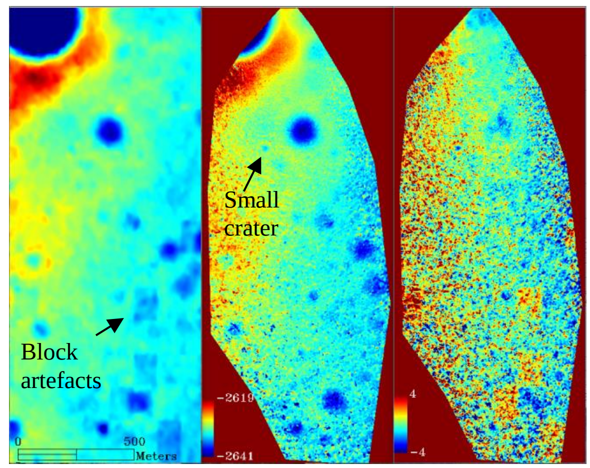

Figure 2. DTM reconstructed with all images. Left: LRO reference, middle : our DTM from CE3 images, right : height difference.

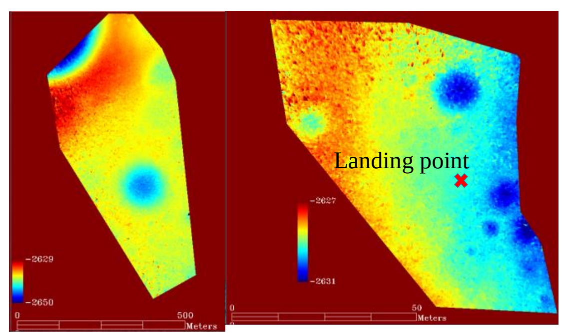

Figure 3. Left : DTM built with images acquired from 800m to 120m height. Right : DTM built with images acquired from 115m to 7m height.

References: [1] https://www.teamindus.in [2] M. S. Menon, A. Kothandhapani et al. (2018) *SpaceOps Conference, Marseille*, Abstract #2494. [3] H. Hirschmüller (2008), *IEEE Trans. Pattern Anal. Mach. Intell.*, 30 (2) [4] C. Li, J. Liu, X. Ren et al. (2015) *Space Sci Rev* (2015) 190: 85. [5] Rupnik et al. (2017) *M. Open geospatial data, softw. stand*, 2:14. [6] Liu Z Q, Di K C, Peng M (2014) *Sci China-Phys Mech Astron*. [7] H.Zhang, et al. (2014) *Scientia Sinica Technologica* 44: 559 [8] Jian-Jun Liu et al, *RAA* (2014) 14:12.